

Nuclear structure and β -decay schemes for Te nuclides beyond $N = 82$

B. Moon,¹ C.-B. Moon,^{2,*} P.-A. Söderström,^{3,†} A. Odahara,⁴ R. Lozeva,^{5,6} B. Hong,¹ F. Browne,^{3,7} H. S. Jung,⁸ P. Lee,⁸ C. S. Lee,⁸ A. Yagi,⁴ C. Yuan,⁹ S. Nishimura,³ P. Doornenbal,³ G. Lorusso,³ T. Sumikama,³ H. Watanabe,³ I. Kojouharov,¹⁰ T. Isobe,³ H. Baba,³ H. Sakurai,³ R. Daido,⁴ Y. Fang,⁴ H. Nishibata,⁴ Z. Patel,^{3,11} S. Rice,^{3,11} L. Sinclair,^{3,12} J. Wu,^{3,13} Z. Y. Xu,¹⁴ R. Yokoyama,¹⁵ T. Kubo,³ N. Inabe,³ H. Suzuki,³ N. Fukuda,³ D. Kameda,³ H. Takeda,³ D. S. Ahn,³ Y. Shimizu,³ D. Murai,¹⁶ F. L. Bello Garrote,¹⁷ J. M. Daugas,¹⁸ F. Didierjean,⁵ E. Ideguchi,¹⁹ T. Ishigaki,⁴ S. Morimoto,⁴ M. Niikura,^{3,14} I. Nishizuka,²⁰ T. Komatsubara,³ Y. K. Kwon,²¹ and K. Tshoo²¹

¹Department of Physics, Korea University, Seoul 136-701, Republic of Korea

²Department of Display Engineering, Hoseo University, Chung-Nam 336-795, Republic of Korea

³RIKEN Nishina Center, Wako, Saitama 351-0198, Japan

⁴Department of Physics, Osaka University, Osaka 560-0043, Japan

⁵IPHC, CNRS, IN2P3, and University of Strasbourg, F-67037 Strasbourg Cedex 2, France

⁶CSNSM, CNRS/IN2P3, University Paris-Sud, F-91405 Orsay Campus, France

⁷School of Computing Engineering and Mathematics, University of Brighton, Brighton BN2 4GJ, The United Kingdom

⁸Department of Physics, Chung-Ang University, Seoul 156-756, Republic of Korea

⁹Sino-French Institute of Nuclear Engineering and Technology, Sun Yat-Sen University, Zhuhai 519-082, China

¹⁰GSI Helmholtzzentrum für Schwerionenforschung GmbH, D-64291 Darmstadt, Germany

¹¹Department of Physics, University of Surrey, Guildford GU2 7XH, The United Kingdom

¹²Department of Physics, University of York, Heslington, York YO10 5DD, The United Kingdom

¹³School of Physics and State Key Laboratory of Nuclear Physics and Technology, Peking University, Beijing 100871, China

¹⁴Department of Physics, University of Tokyo, Tokyo 113-0033, Japan

¹⁵Center for Nuclear Study, University of Tokyo, RIKEN Campus, Wako, Saitama 351-0198, Japan

¹⁶Department of Physics, Rikkyo University, Tokyo 172-8501, Japan

¹⁷Department of Physics, University of Oslo, Oslo N-0316, Norway

¹⁸CEA, DAM, DIF, F-91297 Arpajon Cedex, France

¹⁹RCNP, Osaka University, Osaka 567-0047, Japan

²⁰Department of Physics, Tohoku University, Sendai, Miyagi 980-8578, Japan

²¹Rare Isotope Science Project, Institute for Basic Science, Daejeon 305-811, Republic of Korea

(Received 24 September 2016; revised manuscript received 1 April 2017; published 25 April 2017)

We study for the first time the internal structure of ^{140}Te through the β -delayed γ -ray spectroscopy of ^{140}Sb . The very neutron-rich ^{140}Sb nuclei with $Z = 51$ and $N = 89$ were produced by the in-flight fission of ^{238}U beams at the Radioactive Isotope Beam Factory, RIKEN. The half-life and spin-parity of ^{140}Sb are reported as 173 ± 12 ms and 3^- , respectively. In addition to the excited states of ^{140}Te produced by the β -decay branch, the β -delayed one-neutron and two-neutron emission branches were also established. By identifying the first 2^+ and 4^+ excited states of ^{140}Te , we found that Te isotopes persist in their vibrator character with $E(4^+)/E(2^+) = 2$. We discuss the distinctive features manifest in this region revealed in pairs of isotopes with the same neutron holes and particles with respect to $N = 82$.

DOI: [10.1103/PhysRevC.95.044322](https://doi.org/10.1103/PhysRevC.95.044322)

I. INTRODUCTION

The shell structure of the atomic nucleus is one of the cornerstones for a comprehensive understanding of the many-body quantum system. Fundamental characteristics of nuclear structure are best represented by systematic changes of experimental observables across the nuclear chart [1–4]. Especially, the systematics of the first 2^+ excited states of isotopic and isotonic chains that span the major shell closures are important. Figure 1(a) illustrates such systematics of the even-even $46 \leq Z \leq 54$; it shows clear correlations between the ^{52}Te - ^{48}Cd isotopic chains [4].

The structure of $N > 82$ Te with two protons beyond $Z = 50$ nuclei is expected to provide a wealth of information on the shell evolution of nuclei at extreme proton-neutron ratios. Particular to these nuclei is the impact of the interactions of the two valence protons with the valence neutrons on the overall shell structure. Below $N = 82$, Te isotopes exhibit a typical vibrational character, where coexisting single-particle and collective structures are manifest [9–15]. This vibrational character is found even in ^{136}Te with $N = 84$ [16]. However, the reduction of the energy of its 2_1^+ state in comparison to the $N < 82$ isotopes, as shown in Fig. 1(a), suggests the onset of a stabilized ground-state deformation [17,18], which is predicted to be prolate by Refs. [19] and [20]. Despite this relatively low 2^+ energy, a Coulomb excitation study of ^{136}Te reported an unexpectedly low reduced $E2$ transition strength [21], which contradicts the predicted deformation.

*cbmoon@hoseo.edu

†pasoder@ribf.riken.jp

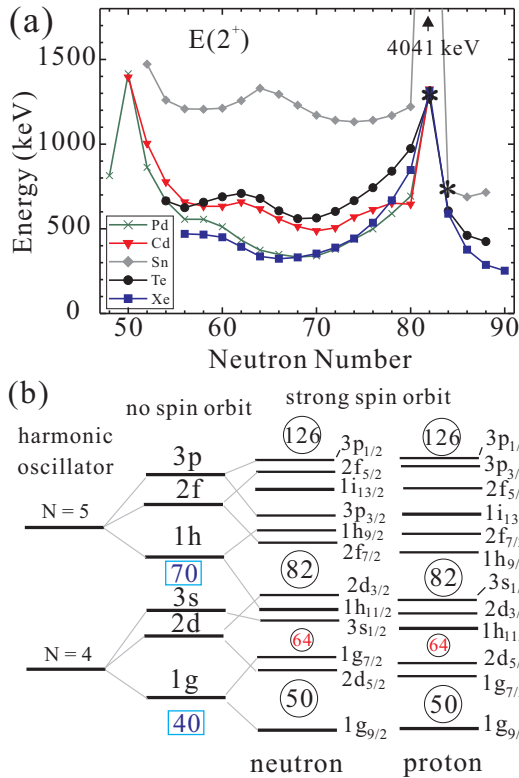


FIG. 1. (a) Systematics of the first 2^+ excited states in the nuclides around Sn ($Z = 50$) as a function of neutron number [4]. Data are primarily from Refs. [5] and [6] for $^{126,128}\text{Pd}$, Ref. [7] for $^{136,138}\text{Sn}$, Ref. [8] for ^{138}Te , and the present work for ^{140}Te . For discussion, the isobars ^{134}Sn and ^{134}Te are emphasized by asterisks (*). (b) The spherical shell-model energy levels of interest in the present work. The numbers at the energy gaps are the subtotals of the number of particles represented by $N_j = 2j + 1$ of identical particles that can occupy each state.

The discrepancy was explained by the quasiparticle random-phase approximation as a neutron-pairing reduction [22] and by the Monte Carlo shell model as neutron dominance through asymmetric proton-neutron couplings [23]. Furthermore, a large-scale shell model calculation also pointed out the importance of the neutron dominance in the wave function of excited states in neutron-rich Te isotopes [24]. A recent study [8] showed that the ratio of the first 4^+ to 2^+ energies, $E(4^+)/E(2^+)$, for ^{138}Te , with $N = 86$, is identical to that of ^{130}Te , with $N = 78$. The energy ratios show a symmetric pattern in Te isotopes with the same valence neutron holes and particles with respect to $N = 82$. Here we address the following questions: (i) does the first 2^+ level energy decrease continuously at $N = 88$ as it does between $N = 84$ (607 keV) and $N = 86$ (461 keV) and (ii) how does the value of $E(4^+)/E(2^+)$ develop at $N = 88$, i.e., does it remain ~ 2 or does it increase? The present work provides crucial experimental data to answer those questions. In this work, we report on the first observation of excited states of ^{140}Te populated by the decay of ^{140}Sb . In addition, we present the β -delayed one- and two-neutron emission schemes.

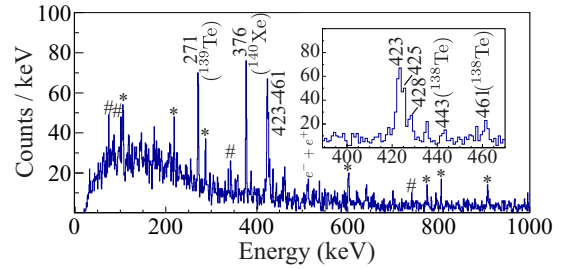


FIG. 2. Single γ -ray spectrum associated with the β decay of ^{140}Sb obtained in the time interval of 2000 ms after ions are implanted on the active target. The inset is a zoomed spectrum from 380 to 470 keV. Peaks with asterisk (*) are room- and beam-induced backgrounds from random coincidence with β events. Peaks with sharp symbols (#) represent unassigned γ rays after decays of Te nuclides.

II. EXPERIMENT AND ANALYSIS

The experiment was carried out at the Radioactive Isotope Beam Factory (RIBF) of the RIKEN Nishina Center. The parent nuclides of ^{140}Te , ^{140}Sb , were produced from the in-flight fission of a 345 MeV per nucleon ^{238}U beam impinging on a ^9Be target and selected by the first stage of the BigRIPS separator [25]. The mean intensity of the primary beam was 5 to 7 pA over the course of the 5 days of beam time. Fission fragments, transported through the BigRIPS and Zero-Degree spectrometers, were unambiguously identified by the $B\rho$ - ΔE -time-of-flight method [26]. These were implanted into the wide-range active silicon strip stopper array for β and ion detection (WAS3ABi), which comprised five layers of 1-mm-thick double-sided silicon-strip detectors [27]. A total of 7.8×10^3 ions of ^{140}Sb were collected amongst $\sim 10^7$ total cocktail beams. Emitted γ rays, following the β decay of ^{140}Sb , were then detected by the EUROBALL-RIKEN high-purity germanium cluster array (EURICA) [28] surrounding WAS3ABi.

Figure 2 shows the β -delayed γ -ray spectrum of ^{140}Sb for events, whose β -decay occurred no later than 2000 ms after the ion implantation. A broad peak in the energy region around 425 keV is visible. The inset of Fig. 2 shows the detailed structure of the spectrum around 425 keV, and, in fact, three peaks are observed at 423-, 425-, and 428-keV transition energies. They are discussed later, in connection with the inset of Fig. 3(b). The strong 271-keV peak observed in Fig. 2 is known to be a transition from the $9/2^-$ state to the ground state in ^{139}Te [5]. This full-energy peak is due to the β -delayed single-neutron emission process, thus the half-life of ^{140}Sb was deduced not only from 423- and 425-keV but also from 271 keV, which is explained later in the inset of Fig. 3(b). Other peaks in Fig. 2 are originated from unassigned γ rays after decays of Te nuclides and random coincidence of room- or beam-induced backgrounds with β rays. Especially, a strong full-energy peak of ^{140}Xe at 376 keV is not only from the decay of ^{140}I but also from the beam-induced background. Unassigned energy peaks marked by sharp symbols (#) are strong candidates for contributions from ^{140}I due to the different aspect of the decay curve, which is coming from the β decay of daughter nuclei.

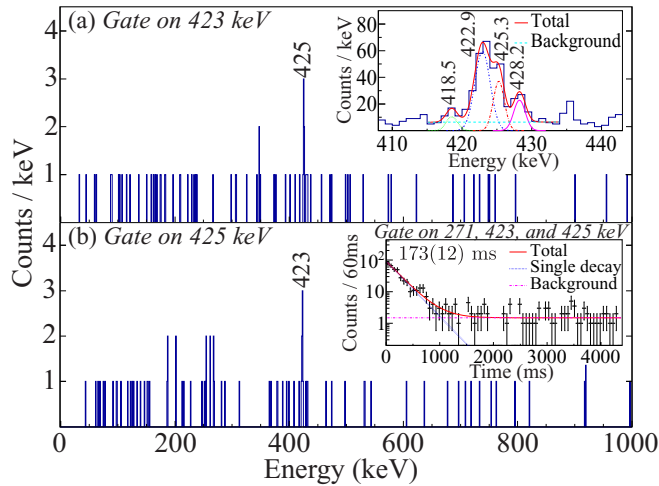


FIG. 3. Coincidence γ -ray spectra gated on (a) 423 keV and (b) 425 keV, which are assigned to the transitions in ^{140}Te . The inset of panel (a) shows the β -delayed singles spectra around 423 keV and their individual peaks fitted by Gaussian function and the background. The 418-keV peak stems from the decay of ^{139}Te and ^{139}I . The inset of panel (b) shows a decay curve gated on the 271-, 423-, and 425-keV full-energy peaks. The red solid line represents the fit using an exponential decay curve and the constant background. The red dashed line depicts the exponential decay curve and the red dashed dot line depicts the constant background. The number in parentheses is an error in the last digit.

The results from the γ - γ coincidence analysis are shown in Fig. 3, where the 423- and 425-keV transitions are shown to be in mutual coincidence; no other transitions were correlated with the 423- and 425-keV transitions. In contrast, the 428-keV peak turned out to be independent of the 423- and 425-keV transitions. On the basis of the γ - γ coincidence data and γ -ray intensities in the singles spectra, we propose that the 423- and 425-keV peaks should be assigned as γ -ray transitions in ^{140}Te . The result of the fit of the β -delayed singles spectrum around 423 keV is shown in Fig. 3(a) to deduce the relative intensities for 423- and 425-keV peaks, which are determined to be 100(16) and 45(12)%. Accordingly, the 425- and 423-keV transitions are assigned as 4^+ to 2^+ and 2^+ to 0^+ , respectively, in ^{140}Te . We also show, in the inset of Fig. 3(b), the decay curve gated on the 271-, 423-, and 425-keV peaks based on the γ -time matrix. The quoted decay half-life was determined using a single-component exponential decay with a maximum likelihood method and assuming a constant background level. The decay half-life was measured to be 173 ± 12 ms when gating on the 271-, 423-, and 425-keV transitions. Additionally, the 428-keV peak showed a similar time-decay curve but was too low in yields to extract a half-life value. Thereby, the 428-keV transition could not be assigned unambiguously to ^{139}Te or ^{140}Te . We note, however, that the 428-keV excitation energy, close to the value of the 2^+ state of ^{140}Te , excludes a possibility that this peak is a transition to the ground state in ^{140}Te .

The intensity of the 271-keV γ ray in ^{139}Te from the β -delayed single-neutron emission was found to be about

74(13)% with respect to the γ -ray intensity of 423 keV in ^{140}Te . From this 271-keV transition, the β -delayed single-neutron emission probability is about 23(4)%. Besides, weak γ -ray peaks at 461- and 443-keV in Fig. 2 belong to ^{138}Te [8]. We assigned these two transitions to ^{138}Te produced by β -delayed two-neutron emission. This β - $2n$ branching ratio, based on γ -ray intensities, was found to be about 8%. We emphasize that there is no evidence of direct feeding from the β decay of ^{140}Sb to the ground state of ^{140}Te from a comparison of the number of implants and the associated β - γ coincident events. However, in cases of β -delayed one-neutron emission, such a direct feeding to the ground state cannot be ruled out due to its ground state of $7/2^-$. Therefore, the probability of the delayed neutron emission may be more intense than that obtained in the present work.

According to the feeding pattern observed, the possible spin-parity values of the ground state of ^{140}Sb can be restricted, because β -decay populates excited states up to 4^+ in ^{140}Te , which implies that the ground state is most likely either 3 or 4. Considering the fact that the intensity of the 423-keV transition is stronger than that of the 425-keV transition, the most likely spin-parity of the ground state of ^{140}Sb is 3^- . As shown in Fig. 1(b), a possible β decay of ^{140}Sb to ^{140}Te is expected to be primarily originated from the conversion of a neutron in the $f_{7/2}$ orbital into a proton in the $g_{7/2}$ (or $d_{5/2}$) orbital as a first-forbidden Gamow-Teller transition. Therefore, the negative-parity assignment is based on a possible proton-neutron configuration of $\pi g_{7/2}$ (or $d_{5/2}$) $\nu f_{7/2}$. Furthermore, the deduced $\log ft$ values for the 2^+ state and the 4^+ state, which are 6.03(13) and 6.02(16), respectively, are in reasonable agreement with our assignment 3^- . If we consider any deformation, however, shell structures might be described in terms of the deformed shell-model orbitals like $[N, n_z, \Lambda]\Omega$ in Nilsson configuration instead of the spherical shell orbitals. For instance, at a quadrupole deformation parameter with $\epsilon_2 = 0.1$ in ^{140}Te , it is found that the $f_{7/2}[512]5/2$, $f_{7/2}[541]3/2$, $h_{9/2}[532]3/2$, and $h_{9/2}[521]1/2$ orbitals for neutrons lie close to the ground state while the $g_{7/2}[431]1/2$, $g_{7/2}[422]3/2$, and $d_{5/2}[420]1/2$ orbitals for protons favor in energy of the ground state. It should be noted that, according to the selection rules for the first-forbidden decays, the 4^- assignment cannot be ruled out. The present results for the decay scheme of ^{140}Sb are summarized in Table I, and the resultant decay scheme of ^{140}Sb is shown in Fig. 4.

III. DISCUSSION

The starting point for the discussion is the description of the systematic behavior of the low-lying level properties in the even-even nuclei of interest. A highly illuminating observable that adheres to systematic behavior is the excitation energy ratios of the first 2^+ and 4^+ states, $R = E(4^+)/E(2^+)$. The value of R provides critical information on the nuclear structure, i.e., < 2 for a spherical shape, 2 for a vibrator, and 3.33 for a deformed axial rotor [30,31]. Figure 5(a) illustrates the systematics of R values for a given neutron number (isotones) along $Z = 50$ (Sn) to $Z = 70$ (Yb), while Fig. 5(b) demonstrates their differences, ΔR , between a pair of isotopes with the same number of valence neutron-holes

TABLE I. Summary of the β decay of ^{140}Sb for ^{140}Te , ^{139}Te by one-neutron emission, and ^{138}Te by two-neutron emission. Probabilities for the respective decay branch are based on the γ -ray measurements. Energies are given in keV. The numbers in parentheses are the errors in the last digit.

Nuclides	Level	$\log(ft)^a$	$I_{\beta^-}^a$	Observed γ rays; I_{γ}^b	Spin-parity
^{140}Te	422.9(3)	6.03(13)	17(3)%	422.9(3); 100(16)	$2^+ \rightarrow 0^+$
	848.2(3)	6.02(16)	14(4)%	425.3(3); 45(12)	$4^+ \rightarrow 2^+$
^{139}Te	271.1(2)		23(4)%	271.1(2); 74(13)	$9/2^- \rightarrow 7/2^-$
^{138}Te	460.8(5)		2.0(8)%	460.8(5); 24(11)	$2^+ \rightarrow 0^+$
	903.6(5)		5.6(2.3)%	442.8(5); 17(12)	$4^+ \rightarrow 2^+$

^aThe number of detected β rays from the β decay of ^{140}Sb to ^{140}Te is 3701(71) based on the β -decay curve of ^{140}Sb ions. The Q value is 12 420 keV.

^bThe unassigned 428-keV γ ray is excluded.

and ν -particles with respect to the closed shell $N = 82$. For example, $\Delta R(88-76)$ for $Z = 52$ means the R value difference between ^{140}Te with $N = 88$ and ^{128}Te with $N = 76$. From the R values, we notice the following characteristics: First, for isotones above $N = 82$ a subshell gap at $Z = 64$ is formed. The subshell gap is quite strong with $N = 88$, moderate with $N = 86$, and becomes weak for $N = 84$. Second, the R values of Te isotopes are centered about two values, 2.0 ($N = 76, 78, 86, 88$) and 1.75 ($N = 80, 84$). This is quite a striking result that is not expected by the present theoretical or empirical predictions, for instance, Ref. [24] in which ^{140}Te is described as a triaxial rotator with $R = 2.33$.

The characteristics in the ΔR systematics can be summarized as follows: (i) There is little difference in the R values in Te, giving $\Delta R \sim 0$. (ii) The ΔR values are constant at $\Delta R \sim -0.175$ for Sn. (iii) They split into the three regimes for Xe and Ba: positive, close to zero, and negative. (iv) The ΔR value distributions have two branches which extend into the negative region for Ce ($Z = 58$) to Dy ($Z = 66$). (v) Finally, a distinctive peak can be found at $Z = 56$ and a

valley structure is pronounced at $Z = 64$ for $\Delta R(88-76)$. This feature provides further confirmation of the existence of a subshell closure at $Z = 64$, strongly reinforced by $N = 88$. The above phenomenological arguments indicate that there is no evidence of the associated change for nuclear structure with deformation between $N = 76$ and $N = 88$ for Te. In other words, Te isotopes give a symmetric signature where the same valence space results in a similar collectivity. In contrast, an emergence of only negative values of ΔR indicates that Sn isotopes above $N = 82$ are less deformed than those below $N = 82$. The Ba isotopes show a greater deformation with $N = 88$ while ^{140}Ba with $N = 84$ is less deformed than its counterpart below $N = 82$, and ^{142}Ba with $N = 86$ has the same deformation as ^{134}Ba with $N = 78$. The Xe isotopes follow similar systematics as Ba. It is worthwhile

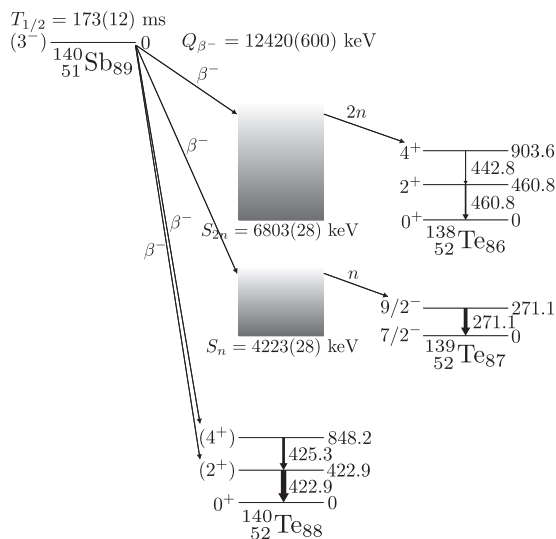


FIG. 4. β -decay scheme of ^{140}Sb deduced from the present work. The Q_{β^-} , S_n , and S_{2n} values are quoted from Ref. [29]. The thicknesses of transitions represent the relative intensities to the 423-keV transition.

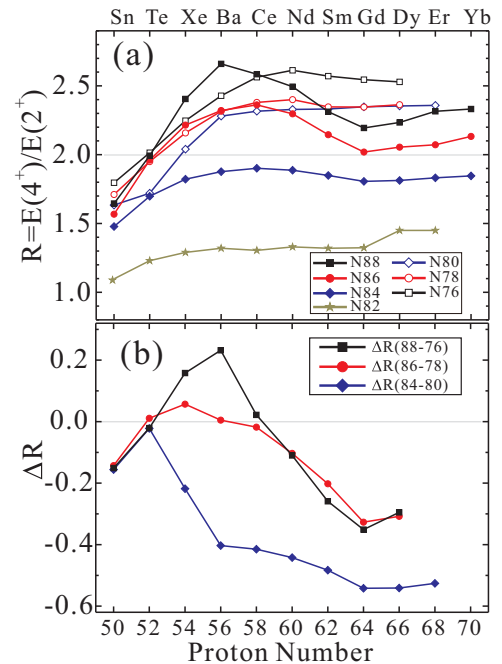


FIG. 5. (a) $R [= E(4^+)/E(2^+)]$ values as a function of proton number in isotopes between $N = 76$ and 88 and (b) ΔR correlations for a pair of isotopes with the same number of valence neutron holes and particles with respect to the closed shell of $N = 82$.

to emphasize that the proton subshell which consists of $g_{7/2}$ and $d_{5/2}$ has a capacity of 14 protons (7 pairs of protons). Given that half-filled, high- j orbitals drive nuclear deformation, Ba ($Z = 56$) and Ce ($Z = 58$) are expected to have maximal deformations. As shown in Fig. 5, this explains why ^{144}Ba and ^{144}Ce have a maximum value of R at $N = 88$ and 86, respectively.

The reduction of neutron-pairing energy can be explained in terms of a large difference between the proton and neutron gap in $^{134}\text{Te}_{82}$ and $^{134}\text{Sn}_{82}$, denoted by stars in Fig. 1(a). Such features for the neutron-rich nuclei above $N = 82$ are also illuminated by the energy difference $\Delta E(2^+)$ between the 2^+ states in a pair of isotopes below and above $N = 82$. For example, the $\Delta E(2^+)$ values for a pair of isotopes of Sn and Te nuclei are found to be 495 : 368, 481 : 379, and 426 : 320 (all in keV) for $N = 80 : 84$, $N = 78 : 86$, and $N = 76 : 88$, respectively. As already pointed out in case of ^{136}Te , neutron dominance in the 2^+ state leads to a weaker $B(E2)$ value [21]. Interestingly, the $\Delta E(2^+)$ values are almost the same within 10% for both Sn and Te. This result implies that the neutron pairings at $N = 86$ and 88 are likely comparable to that at $N = 84$. On the contrary, the ΔR values indicate that the Te isotopes maintain their collective character, showing $\Delta R \approx 0$ over the $N = 82$ shell closure for a typical vibrator. A sophisticated shell-model theory, employing the proton-neutron mixed asymmetric interactions, is required for an understanding of the underlying physics in ^{140}Te .

IV. CONCLUSION

In conclusion, we provide the first data of the β -decay scheme of the very neutron-rich ^{140}Sb and the excited states

of its daughter nucleus, ^{140}Te . The half-life and spin-parity of ^{140}Sb were measured to be 173(12) ms and 3^- , respectively. We identified β decay, β -delayed one-neutron emission, and β -delayed two-neutron emission from the decay of ^{140}Sb and determined their decay probabilities on the basis of γ -ray measurements involved in each daughter nucleus. We deduced the first 2^+ and 4^+ excited states in ^{140}Te , indicating $E(4^+)/E(2^+) \sim 2$ seen in other isotopes. We discussed the level structure of ^{140}Te based on the systematics of the 2^+ and 4^+ states in the vicinity of $N = 82$. Along with the study of Te isotopes, we addressed some interesting aspects by focusing on the distinctive features of nuclides from Sn ($Z = 50$) to Yb ($Z = 70$).

ACKNOWLEDGMENTS

This work was carried out at the RIBF operated by RIKEN Nishina Center, RIKEN, and CNS, University of Tokyo. We acknowledge the EUROBALL Owners Committee for the loan of germanium detectors and the PreSpec Collaboration for the readout electronics of the cluster detectors. Part of the WAS3ABi was supported by the Rare Isotope Science Project, which is funded by the Ministry of Science, ICT and Future Planning (MSIP), and the National Research Foundation (NRF) of Korea. This research was partly supported by JSPS KAKENHI Grant No. 25247045 and National Research Foundation grants funded by the Korea Government (Grants No. NRF-2009-0093817, No. NRF-2013R1A1A2063017, No. NRF-2016K1A3A7A09005575, and No. NRF-2016K1A3A7A09005578). The FR-JP LIA support is also acknowledged.

-
- [1] K. Heyde, P. van Isacker, M. Waroquier, J. L. Wood, and R. A. Meyer, *Phys. Rep.* **102**, 291 (1983).
 - [2] J. L. Wood, K. Heyde, W. Nazarewicz, M. Huyse, and P. van Duppen, *Phys. Rep.* **215**, 101 (1992).
 - [3] K. Heyde and J. L. Wood, *Rev. Mod. Phys.* **83**, 1467 (2011).
 - [4] C.-B. Moon, *AIP Adv.* **4**, 041001 (2014).
 - [5] National Nuclear Data Center, Brookhaven National Laboratory, www.nndc.bnl.gov/.
 - [6] H. Watanabe *et al.*, *Phys. Rev. Lett.* **111**, 152501 (2013).
 - [7] G. S. Simpson *et al.*, *Phys. Rev. Lett.* **113**, 132502 (2014).
 - [8] P. Lee *et al.*, *Phys. Rev. C* **92**, 044320 (2015).
 - [9] J. J. Van Ruyven, W. H. A. Hesselink, J. Akkermans, P. Van Nes, and H. Verheul, *Nucl. Phys. A* **380**, 125 (1982).
 - [10] M. Sambataro, *Nucl. Phys. A* **380**, 365 (1982).
 - [11] J. Rikovska, N. J. Stone, and W. B. Walters, *Phys. Rev. C* **36**, 2162 (1987).
 - [12] C. S. Lee, J. A. Cizewski, D. Barker, R. Tanczyn, G. Kumbartzki, J. Szczepanski, J. W. Gan, H. Dorsett, R. G. Henry, and L. P. Farris, *Nucl. Phys. A* **528**, 381 (1991).
 - [13] C.-B. Moon, J. U. Kwon, S. J. Chae, J. C. Kim, S. H. Bhatti, C. S. Lee, T. Komatsubara, J. Mukai, T. Hayakawa, H. Kimura, J. Lu, M. Matsuda, T. Watanabe, and K. Furuno, *Phys. Rev. C* **51**, 2222 (1995).
 - [14] C.-B. Moon, T. Komatsubara, T. Shizuma, K. Uehiyama, N. Hashimoto, M. Katoh, K. Matsuura, M. Murasaki, Y. Sasaki, H. Takahashi, Y. Tokita, and K. Furuno, *Z. Phys. A* **358**, 373 (1997).
 - [15] C.-B. Moon, S. J. Chae, T. Komatsubara, T. Shizuma, Y. Sasaki, H. Ishiyama, T. Jumatsu, and K. Furuno, *Nucl. Phys. A* **657**, 251 (1999).
 - [16] J. A. Cizewski, M. A. C. Hotchkis, J. L. Durell, J. Copnell, A. S. Mowbray, J. Fitzgerald, W. R. Phillips, I. Ahmad, M. P. Carpenter, R. V. F. Janssens, T. L. Khoo, E. F. Moore, L. R. Morss, Ph. Benet, and D. Ye, *Phys. Rev. C* **47**, 1294 (1993).
 - [17] R. O. Hughes, N. V. Zamfir, R. F. Casten, D. C. Radford, C. J. Barton, C. Baktash, M. A. Caprio, A. Galindo-Uribarri, C. J. Gross, P. A. Hausladen, E. A. McCutchan, J. J. Ressler, D. Shapira, D. W. Stracener, and C.-H. Yu, *Phys. Rev. C* **69**, 051303(R) (2004).
 - [18] M. Danchev, G. Rainovski, N. Pietralla, A. Gargano, A. Covello, C. Baktash, J. R. Beene, C. R. Bingham, A. Galindo-Uribarri, K. A. Gladnishki, C. J. Gross, V. Yu. Ponomarev, D. C. Radford, L. L. Riedinger, M. Scheck, A. E. Stuchbery, J. Wambach, C.-H. Yu, and N. V. Zamfir, *Phys. Rev. C* **84**, 061306(R) (2011).

- [19] F. Hoellinger, B. J. P. Gall, N. Schulz, W. Urban, I. Ahmad, M. Bentaleb, J. L. Durell, M. A. Jones, M. Leddy, E. Lubkiewicz, L. R. Morss, W. R. Phillips, A. G. Smith, and B. J. Varley, *Eur. Phys. J. A* **6**, 375 (1999).
- [20] W. Urban, W. R. Phillips, N. Schulz, B. J. P. Gall, I. Ahmad, M. Bentaleb, J. L. Durell, M. A. Jones, M. J. Leddy, E. Lubkiewicz, L. R. Morss, A. G. Smith, and B. J. Varley, *Phys. Rev. C* **62**, 044315 (2000).
- [21] D. C. Radford, C. Baktash, J. R. Beene, B. Fuentes, A. Galindo-Uribarri, C. J. Gross, P. A. Hausladen, T. A. Lewis, P. E. Mueller, E. Padilla, D. Shapira, D. W. Stracener, C.-H. Yu, C. J. Barton, M. A. Caprio, L. Coraggio, A. Covello, A. Gargano, D. J. Hartley, and N. V. Zamfir, *Phys. Rev. Lett.* **88**, 222501 (2002).
- [22] J. Terasaki, J. Engel, W. Nazarewicz, and M. Stoitsov, *Phys. Rev. C* **66**, 054313 (2002).
- [23] N. Shimizu, T. Otsuka, T. Mizusaki, and M. Honma, *Phys. Rev. C* **70**, 054313 (2004).
- [24] D. Bianco, N. Lo Iudice, F. Andreozzi, A. Porrino, and F. Knapp, *Phys. Rev. C* **88**, 024303 (2013).
- [25] T. Kubo, D. Kameda, H. Suzuki, N. Fukuda, H. Takeda, Y. Yanagisawa, M. Ohtake, K. Kusaka, K. Yoshida, N. Inabe, T. Ohnishi, A. Yoshida, K. Tanaka, and Y. Mizoi, *Prog. Theor. Exp. Phys.* **2012**, 03C003 (2012).
- [26] N. Fukuda, T. Kubo, T. Ohnishi, N. Inabe, H. Takeda, D. Kameda, and H. Suzuki, *Nucl. Instrum. Methods Phys. Res., Sect. B* **317**, 323 (2013).
- [27] S. Nishimura, *Prog. Theor. Exp. Phys.* **2012**, 03C006 (2012).
- [28] P.-A. Söderström *et al.*, *Nucl. Instrum. Methods Phys. Res., Sect. B* **317**, 649 (2013).
- [29] M. Wang, G. Audi, A. H. Wapstra, F. G. Kondev, M. MacCormik, X. Xu, and B. Pfeiffer, *Chin. Phys. C* **36**, 1603 (2012).
- [30] R. F. Casten, D. D. Warner, D. S. Brenner, and R. L. Gill, *Phys. Rev. Lett.* **47**, 1433 (1981).
- [31] R. B. Cakirli and R. F. Casten, *Phys. Rev. C* **78**, 041301(R) (2008).